


RESEARCH ARTICLE

Long-term Musculoskeletal Consequences of Chemotherapy in Pediatric Mice

Joshua R. Huot^{1,2,3,4,†}, Patrick D. Livingston^{4,†}, Fabrizio Pin^{1,2,3}, Connor R. Thomas¹, Nicholas A. Jamnick⁵, Chandler S. Callaway⁵, Andrea Bonetto ^{5,6,*}

¹Department of Anatomy, Cell Biology and Physiology, Indiana University School of Medicine, Indianapolis, IN, 46202 USA, ²Simon Comprehensive Cancer Center, Indiana University School of Medicine, Indianapolis, IN, 46202 USA, ³Indiana Center for Musculoskeletal Health, Indiana University School of Medicine, Indianapolis, IN, 46202 USA, ⁴Department of Kinesiology, School of Health and Human Sciences, Indiana University Purdue University Indianapolis, IN, 46202 USA, ⁵Department of Pathology, University of Colorado Anschutz Medical Campus, Aurora, CO, 80045 USA and ⁶University of Colorado Comprehensive Cancer Center, University of Colorado Anschutz Medical Campus, Aurora, CO, 80045 USA

*Address correspondence to A.B. (e-mail: andrea.bonetto@cuanschutz.edu)

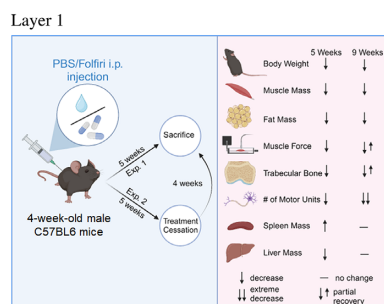
[†]Joshua R. Huot and Patrick D. Livingston contributed equally to this work.

Abstract

Thanks to recent progress in cancer research, most children treated for cancer survive into adulthood. Nevertheless, the long-term consequences of anticancer agents are understudied, especially in the pediatric population. We and others have shown that routinely administered chemotherapeutics drive musculoskeletal alterations, which contribute to increased treatment-related toxicity and long-term morbidity. Yet, the nature and scope of these enduring musculoskeletal defects following anticancer treatments and whether they can potentially impact growth and quality of life in young individuals remain to be elucidated. Here, we aimed at investigating the persistent musculoskeletal consequences of chemotherapy in young (pediatric) mice. Four-week-old male mice were administered a combination of 5-FU, leucovorin, irinotecan (*a.k.a.*, Folfiri) or the vehicle for up to 5 wk. At time of sacrifice, skeletal muscle, bones, and other tissues were collected, processed, and stored for further analyses. In another set of experiments, chemotherapy-treated mice were monitored for up to 4 wk after cessation of treatment. Overall, the growth rate was significantly slower in the chemotherapy-treated animals, resulting in diminished lean and fat mass, as well as significantly smaller skeletal muscles. Interestingly, 4 wk after cessation of the treatment, the animals exposed to chemotherapy showed persistent musculoskeletal defects, including muscle innervation deficits and abnormal mitochondrial homeostasis. Altogether, our data support that anticancer treatments may lead to long-lasting musculoskeletal complications in actively growing pediatric mice and support the need for further studies to determine the mechanisms responsible for these complications, so that new therapies to prevent or diminish chemotherapy-related toxicities can be identified.

Submitted: 29 November 2023; Revised: 8 February 2024; Accepted: 4 March 2024

© The Author(s) 2024. Published by Oxford University Press on behalf of American Physiological Society. This is an Open Access article distributed under the terms of the Creative Commons Attribution-NonCommercial License (<https://creativecommons.org/licenses/by-nc/4.0/>), which permits non-commercial re-use, distribution, and reproduction in any medium, provided the original work is properly cited. For commercial re-use, please contact journals.permissions@oup.com



Key words: chemotherapy; Folfiri; skeletal muscle; bone mass; mouse models; long-term consequences

Introduction

The overall mortality rate for childhood and adolescent cancers has been decreasing steadily by an average of 2.1% since the 1970s due to improvements in anti-cancer therapies, diagnostic equipment, and access to medical care, allowing most diagnosed children to survive into adulthood.^{1,2} Brain tumors alongside leukemia are some of the most common as well as deadliest cancer types for children and adolescents.² These kinds of cancer also present the highest risk for long-term complications due to the intensity of anti-cancer therapy.¹ While these treatments have drastically increased the survival rates, they remain toxic in nature, and elicit consequential side effects in the body.^{3,4} While the immediate side effects of chemotherapy on skeletal muscle and bone are well studied, little is known about the longstanding consequences of these anti-cancer agents, especially in the pediatric population. With a steadily increasing survival rate for diagnosed children, and a lack of infrastructure to properly study pediatric populations, understanding the long-term effects of treatment is becoming more important than ever.⁵

Chemotherapeutic agents act primarily by disrupting essential mechanisms of cell division and have a high biological activity that can lead to the eradication of cancer cells.⁶ This increased activity is multifarious and not entirely isolated to cancerous cells, which can elicit a toxic response in the host. Side effects can include nausea, vomiting, diarrhea, anorexia, body weight changes, anemia, and muscle weakness and fatigue.⁷ As we and others have shown in the recent past, musculoskeletal alterations induced by chemotherapy are analogous with symptoms of “cancer-induced cachexia.”^{8,9} Cachexia can be described as a multifactorial wasting syndrome marked by loss in skeletal muscle mass, appetite, and weight, altogether leading to fatigue, a poor quality of life (QoL), perturbations in metabolism, and overall decreased survival rate.^{3,10-11} Cachexia promoted by cancer is exacerbated and compounded through the application of anti-cancer therapies, leading to increased mortality.⁸ Upwards of 80% of all adult cancer patients will experience cachexia, which is directly responsible for 30% of all cancer related deaths.¹²⁻¹⁵ Defining cachexia for the pediatric population is much more difficult because of the physiological differences with puberty and age as well as the presence of reporting bias through parents for children and adolescents.^{5,16} Through the application of in vivo animal models as well as clinical trial studies, we have begun to understand the consequential side effects of certain anti-cancer therapies, but there is a lack of data surrounding how those effects can persist throughout the patient’s life.

Studies in healthy rats have demonstrated that chemotherapies such as cyclophosphamide, 5-fluorouracil, cisplatin, and

methotrexate induce a negative nitrogen balance and commensurate weight loss.⁹ Research from our laboratory exploring the combination therapy 5-fluorouracil, leucovorin, and irinotecan (a chemotherapy regimen known as Folfiri) has shown that wasting is dependent upon activation of ERK1/2 and p38 mitogen-activated protein kinases pathways but, unlike cancer-associated cachexia, is independent of the ubiquitin proteasome system.¹⁷ It is becoming more recognized that cachexia is a metabolic disorder that cannot be corrected by increased food intake alone.^{8,17-20} Oxidative stress has also been identified as a consequence of a number of chemotherapeutic agents, which could induce muscle wasting via mitochondrial dysfunction.^{4,8,17,21,22} These studies highlight the complexity of the muscle wasting effects of chemotherapy and suggest that more detailed studies are needed to elucidate the systems that drive both cancer-associated and chemotherapy-induced cachexia. None of these models, however, examine the intricacies of how these drugs affect a developing body and/or attempt to unravel the long-term consequences of exposure to these drugs in young individuals.

Here, we investigated the lasting musculoskeletal effects of Folfiri, a commonly used combination chemotherapeutic drug that our group has extensively characterized.^{3,8,15,17,23,24} Four-week-old male C57BL6/J mice were administered either chemotherapy or the vehicle IP for up to 5 wk. In order to accurately measure recovery, another experiment was done with age-matched mice that were administered chemotherapy for 5 wk and followed for up to 4 wk after cessation of the treatment. Body composition, plantarflexion torque, food intake, and indices of motor unit connectivity were assessed at baseline and at regular intervals. At time of sacrifice, skeletal muscle, bones, and other tissues were collected, processed, and stored for further analyses.

Materials and Methods

Animals

All in vivo experiments were approved by the Institutional Animal Care and Use Committee at Indiana University School of Medicine and were in compliance with the National Institutes of Health Guidelines for Use and Care of Laboratory Animals. To examine the effects of chemotherapy on the musculoskeletal system of pediatric mice, 4-wk-old C57BL/6J male mice (The Jackson Laboratory, Bar Harbor, ME, USA) were randomized into 2 groups based off initial body mass and sacrificed at 2 different timepoints (Figure S1). A first group of animals was administered Folfiri (5-FU, 50 mg/kg; leucovorin, 90 mg/kg; irinotecan, 24 mg/kg, 2 h post 5-FU and leucovorin; solubilized in DMSO;

$n = 10$; C; 200 μL) intraperitoneally (IP), twice weekly for up to 5 wk, whereas the control mice ($n = 5$; V) were administered an isovolumetric IP injection of vehicle (sterile PBS solution and DMSO) following the same dosing schedule.¹⁷ A second group of mice received Folfiri for 5 wk, followed by 4 wk of monitoring before being euthanized at 13 wk of age. All mice were given injections at identical volumes (200 μL) and frequencies. Animal weight and food intake were monitored daily. Body composition, in vivo plantarflexion torque, and indices of motor unit connectivity were all assessed at baseline and at regular intervals (Figure S1). At time of euthanasia, skeletal muscles (gastrocnemius, quadriceps, tibialis anterior) and other organs (heart, liver, spleen, epididymal fat, and kidneys) were harvested, weighed, and snap frozen, while the extensor digitorum longus (EDL) muscles underwent ex vivo muscle contractility measurement to determine the impact of chemotherapy on muscle function.

Dual-Energy X-Ray Absorptiometry

Assessment of lean tissue, fat mass, as well as whole-body bone mineral density (BMD) and bone mineral content (BMC) was assessed by means of dual-energy x-ray absorptiometry (DEXA) scanning. Mice were scanned at regular intervals over the course of the study (weeks 0, 2, 5, 7, and 9). According to the manufacturer's guidelines, in order to calibrate and validate the apparatus for its performance, a spine phantom was scanned using the Lunar PIXImus densitometer (PIXImus, Fitchburg, WI) before scanning the first mouse. Mice were placed in a prone position with the limbs outstretched and kept under anesthesia using a nose cone and isoflurane. From the whole-body scans, areal BMD, BMC, total fat mass, and total lean mass were calculated for the entire body minus the head ROI using the Lunar ROI tools.

Ex Vivo Muscle Contractility

The contractile force in EDL muscles was measured through whole-muscle contractility assessment. The EDL muscles were quickly dissected in a tray containing Tyrode solution (121 mM NaCl, 5.0 mM KCl, 1.8 mM CaCl₂, 0.5 mM MgCl₂, 0.4 mM NaH₂PO₄, 24 mM NaHCO₃, 0.1 mM EDTA, and 5.5 mM glucose), and stainless-steel hooks were tied to both tendons using 4-0 silk sutures. The muscles were placed between a mounted force transducer (Aurora Scientific, Aurora, ON, Canada) and incubated in a stimulation bath containing Tyrode supplemented with continuous O₂/CO₂ (95/5%). Following a 10-min incubation period, the maximum twitch force was obtained by determining optimal muscle length (L_0), and force–frequency relationships were assessed using a supramaximal incremental frequency stimulation sequence (10, 25, 40, 60, 80, 100, 125, and 150 Hz for 350 ms). Force data were collected and analyzed with the Dynamic Muscle Control/Data Acquisition and Dynamic Muscle Control Data Analysis programs (Aurora Scientific), and EDL muscle weight and L_0 were used to determine specific force.

In Vivo Plantarflexion Torque Assessment

Animals from the 2 experimental cohorts underwent in vivo plantarflexion torque assessment (Aurora Scientific) to assess the impact of chemotherapy on hindlimb muscle torque. Briefly, the left hind foot was taped to the force transducer and positioned to where the foot and tibia were aligned at 90°. The

knee was then clamped at the femoral condyles, avoiding compression of the fibular nerve. Two disposable monopolar electrodes (Natus Neurology, Middleton, WI) were placed subcutaneously, posterior/medial to the knee in order to stimulate the tibial nerve. Maximum twitch torque was first determined using supramaximal stimulations (0.2 ms square wave pulse). Peak plantarflexion torque was then assessed following a supramaximal square wave stimulation (0.2 ms) delivered at a frequency of 100 Hz.

Assessment of Muscle Cross-Sectional Area

To assess skeletal muscle cross-sectional area (CSA), 10 μm -thick cryosections taken at the mid-belly of the tibialis anterior muscle were processed for immunostaining, as described previously.²⁵ Sections were blocked in 8% bovine serum albumin for 1 h at room temperature and incubated at 4°C overnight in dystrophin primary antibody (#MANDRA11 (8B11); Developmental Studies Hybridoma Bank, Iowa City, IA, USA), followed by incubation in secondary antibody (AlexaFlour 555 # A-21127; Thermo Fisher Scientific, Waltham, MA, USA) for 1 hour at room temperature. Sections were then washed, mounted, and imaged using a Lionheart LX automated microscope (BioTek Instruments).

In Vivo Electrophysiology

Triceps surae muscles of all animals were subjected to electrophysiological functional assessment using the Sierra Summit 3–12 Channel EMG (Cadwell Laboratories Incorporated, Kennewick, WA), as performed previously.²⁶ Two 28-gauge stimulating needle electrodes (Natus Neurology, Middleton, WI) were used to stimulate the sciatic nerve of the left hindlimb, a duo shielded ring electrode was used for recording, and a ground electrode was placed over the animal's tail. Baseline-to-peak and peak-to-peak compound muscle action potential (CMAP) responses were recorded utilizing supramaximal stimulations (constant current intensity: <10 mA; pulse duration: 0.1 ms). In addition to CMAP responses, all animals were assessed for peak-to-peak single motor unit potential (SMUP) responses, using the incremental stimulation technique, as previously described.^{26,27} Briefly, the sciatic nerve was sub maximally stimulated until stable, minimal all-or-none responses occurred. Ten successive SMUP increments were recorded and averaged. Baseline-to-peak CMAP amplitudes were used for comparison between experimental groups, and motor unit number estimation (MUNE) was calculated using peak-to-peak CMAP and average SMUP, using the following equation: MUNE = CMAP amplitude (peak-to-peak)/average SMUP (peak-to-peak).

Western Blotting

Protein extracts were obtained by homogenizing 100 mg of quadriceps muscle in RIPA buffer (150 mM NaCl, 1.0% NP-40, 0.5% sodium deoxycholate, 0.1% SDS, and 50 mM Tris, pH 8.0) supplemented with inhibitor cocktails for proteases (Roche, Indianapolis, IN) and phosphatases (Thermo Scientific, Rockford, IL) on ice. Quadriceps muscle was used here to maintain consistency with our previously published studies.^{8,17} Cellular debris was removed via centrifugation (15 min, $\times 14\,000\ g$ at 4°C), and protein concentration was assessed using a BCA Protein Assay Kit (Thermo Scientific). Protein extracts (30 μg) were electrophoresed in 4%–15% gradient SDS Criterion TGX precast gels (Bio-Rad, Hercules, CA) and transferred to nitrocellulose membranes (30 min at 100 V; Bio-Rad). Membranes were blocked

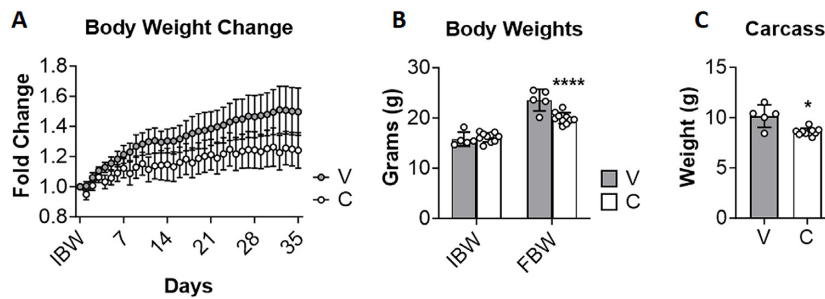


Figure 1. Chemotherapy promotes stunted growth in young mice. (A) Body weight change in mice from experiment #1, normalized to IBW. (B) Final body weights. (C) Carcass weights recorded after dissecting skeletal muscles and organs. Data reported as means \pm SD. Significant differences ($*P < .05$; $**P < .01$; $****P < .0001$) were determined by using 2-way ANOVA and Student's *t*-test.

with Odyssey blocking buffer (LI-COR Biosciences, Lincoln, NE) at room temperature for 1 h and incubated overnight in primary antibodies at 4°C with gentle rocking. Following primary antibody incubation, membranes were washed 3 times with PBS containing 0.2% Tween-20 (PBST), and the membrane was incubated at room temperature for 1 h with either anti-rabbit IgG (H + L) DyLight 800 or anti-mouse IgG (H + L) DyLight 680 secondary antibodies (Cell Signaling Technologies, Danvers, MA). Blots were again washed 3 times using PBST and then visualized with an Odyssey CLx Imaging System (LI-COR Biosciences, Lincoln, NE). Optical density measurements were taken using the ImageJ software.²⁸ Antibodies used were for phospho-p44/42 MAPK (p-ERK1/2; #4370), p44/42 MAPK (ERK1/2; #4695), phospho-p38 MAPK (p-p38; #4511), p38 MAPK (p38; #8690), voltage dependent ion channels (VDAC; #4866), optic atrophy 1 (OPA-1; #80 471), dynamin-related protein 1 (DRP-1; #8570), mitofusin-2 (#9482S), cytochrome C (#11 940), COX IV (#4850) from Cell Signaling Technologies; peroxisome gamma coactivator-1 alpha (PGC-1 α ; #AB3242) was from Millipore-Sigma (Burlington, VA); peroxisome gamma coactivator-1 beta (PGC-1 β ; #ab176328), muscle-specific kinase (MuSK; #ab92950), receptor-associated protein of the synapse (Rapsyn; #ab156002), and downstream-of-kinase 7 (Dok-7; #ab75049) from Abcam (Waltham Boston, MA); and α -tubulin (#12G10) from Developmental Studies Hybridoma Bank (Iowa City, IA).

Succinate Dehydrogenase Enzymatic Activity

The enzymatic activity of succinate dehydrogenase (SDH) was measured in soleus muscle homogenates using Colorimetric Assay Kits (#MAK197) from Sigma-Aldrich according to the manufacturer's instruction. Briefly, 10 mg of skeletal muscle tissue was homogenized in 100 μ L of ice-cold assay buffer and then centrifuged, and 10 μ L of homogenate was added to 96-well plates. Appropriate reaction mix was added to each of the wells and the product of enzyme reaction, which results in a colorimetric (600 nm for SDH) product proportional to the enzymatic activity. The absorbance was recorded by incubating the plate at 37°C taking measurements (600 or 450 nm) every 5 for 30 min.

Micro Computed Tomography

After euthanasia, the right femur was dissected from each mouse, fixed for 2 d in 10% neutral buffered formalin, and then transferred into 70% ethanol for micro computed tomography (μ CT) scanning on a high-throughput μ CT specimen scanner (μ CT-35; Scanco Medical AG). The distal 33% of each bone was

scanned using the following conditions: 50 kV, 120 mA, 151-ms integration time, 0.5 mm Al filter, and 10- μ m voxel resolution.²⁹ Three-dimensional morphometric properties of the distal femur cancellous bone were measured as previously described.³⁰ Briefly, trabecular bone volume fraction (BV/TV; %), trabecular number (Tb.N; 1/ μ m), trabecular thickness (Tb.Th; μ m), trabecular spacing (Tb.Sp; μ m), and connectivity density (Conn.Dn; 1/ μ m³) were determined on a 1.5 mm region of the distal femur secondary spongiosa, using an ROI beginning 0.6 mm proximal to the distal growth plate (identified by radiolucency and morphology) and extending proximally for 1.5 mm. The trabecular bone was digitally isolated from the cortical compartment by manually lassoing the trabecular bone every 15 slices, then interpolating the trabecular compartment in intervening slices using the contouring function in the Scanco software. All measurements were calculated automatically using the Scanco software (μ CT v6.1).

Statistics

All statistical analyses were performed using GraphPad Prism 9.0.0 (GraphPad Software, San Diego, CA, USA). Two-tailed Student's *t*-tests were performed to determine significant differences between vehicle- and chemotherapy-treated animals. A 2-way repeated-measures analysis of variance (ANOVA) was performed, followed by Bonferroni's post hoc comparisons, for longitudinal measures and ex vivo muscle contractility of the EDL. In general, variance was tested throughout our study, and in most cases, there were no significant differences. When a variance was significant, a Welch's test was used. Statistical significance was set at $P \leq .05$, and the data were presented as means \pm SD.

Results

Chemotherapy Promotes Stunted Growth in Young Mice

We and others have shown that chemotherapy treatments can induce and/or exacerbate cancer cachexia symptoms, therefore promoting worsened muscle and bone loss.^{3,4} However, whether these musculoskeletal derangements persist in time even after cessation of the treatments remains to be fully understood. In order to understand the systems associated with persistent chemotherapy-related effects on body composition and muscle function, we must first determine how these defects progressively develop in young mice exposed to anticancer agents. Hence, we treated young (4-wk-old) C57/BL6J mice with vehicle (V) or chemotherapy (C) for up to 5 wk, similar to our previous studies.¹⁷ As shown in **Figure 1A**, the

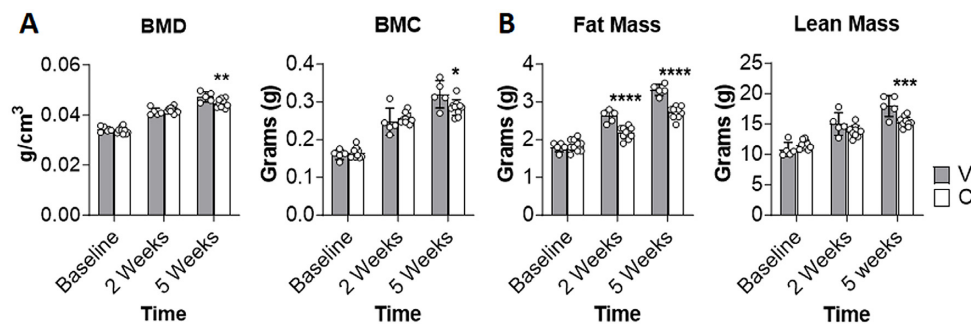


Figure 2. Bone, fat, and muscle mass are blunted during chemotherapy treatment. (A) Total bone mineral density (BMD), bone mineral content (BMC), (B) lean muscle mass, and fat mass assessed by dual-energy x-ray absorptiometry in mice from experiment #1. Data reported as means \pm SD. Significant differences (** $P < .01$; *** $P < .001$) were determined by using 2-way ANOVA.

chemotherapy-treated mice exhibited stunted body weight gain over the 35-d period, thus leading to a 15% body weight difference when compared to the animals receiving the vehicle ($P < .0001$) (Figure 1B), also consistent with significantly smaller carcass weights (-15% , vs. V, $P < .05$) (Figure 1C).

Bone, Fat, and Muscle Mass Are Blunted During Chemotherapy Treatment

We previously reported that chronic administration of Folfiri elicits significant changes in body composition, coherent with marked losses of fat and lean mass and with significant depletion of trabecular bone.^{15,17,23,31} Here, we conducted body composition assessment by means of DEXA (Figure 2) and analogously found that the chemotherapy-administered mice displayed significantly reduced whole-body BMD (-5% , $P < .01$) and BMC (-10% , $P < .05$) vs. V mice after 5 wk of treatment (Figure 2A). It was also observed that the Folfiri-treated animals underwent reduced accumulation of fat mass vs. V mice (Figure 2B), already evident at week 2 and persisting through week 5 (W2: -16% , $P < .0001$; W5: -18% , $P < .0001$). A similar trend was observed in lean muscle gains, which were significantly different in the C mice vs. V mice at week 5 (-14% , $P < .001$).

Chemotherapy Stunts Muscle Growth and Force Production

As shown previously in our lab, adult animals that have undergone chemotherapy treatments show marked skeletal muscle atrophy and weakness (ie, cachexia).^{15,17,31} Here, 4-wk-old mice receiving Folfiri for up to 5 wk exhibited smaller gastrocnemius, quadriceps, and tibialis anterior muscle weights compared to the control animals (-23% , $P < .001$; -23% , $P < .001$; -22% , $P < .001$, respectively) (Figure 3A). In line with our recent findings, chemotherapy also caused significant muscle weakness¹⁵ with in vivo plantarflexion torque assessment in the chemotherapy-treated animals showing a marked reduction in skeletal muscle force generation at weeks 2 and 5 as compared to the controls (W2: -16% , $P = .0259$; W5: -23% , $P < .0001$) (Figure 3B). Similarly, the ex vivo EDL muscle contractility analysis also revealed force reductions in the Folfiri-treated mice at time of sacrifice (-21% at 125 Hz vs. V, $P < .01$) (Figure 3C).

Chemotherapy Profoundly Affects Trabecular Bone

We and others have shown that different chemotherapeutics all drive significant losses of bone mass, consistent with changes in bone volume fraction (BV/TV, indicative of the volume of

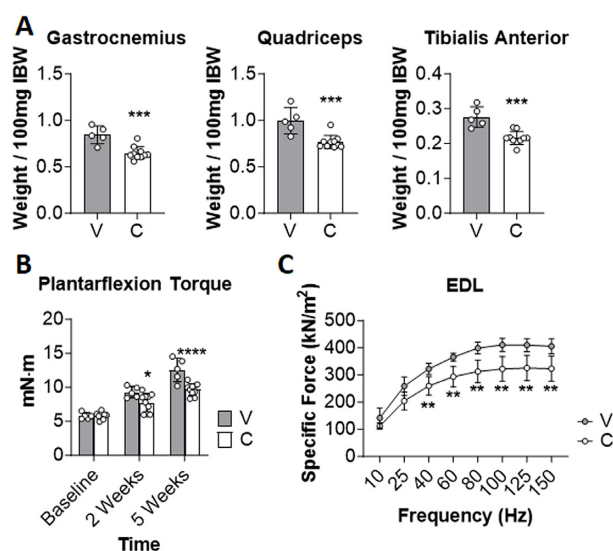


Figure 3. Chemotherapy stunts muscle growth and force production. (A) Skeletal muscle weights from mice enrolled in experiment #1 were normalized to body weight at start of treatment (initial body weight—IBW). (B) In vivo plantarflexion force assessment reported as absolute torque (expressed as mN-m). (C) Ex vivo assessment reported as specific force (kN/m²). Data reported as means \pm SD. Significant differences (* $P < .05$; ** $P < .01$; *** $P < .001$; **** $P < .0001$) were determined by Student's t-test and 2-way ANOVA.

mineralized bone per unit volume of sample), trabecular thickness (Tb.Th, ie, the average thickness of the trabeculae), trabecular number (Tb.N, representing the number of trabeculae per unit of length), connectivity density (Conn.Dn, indicating the trabecular connections per unit of volume) and trabecular spacing (Tb.Sp, a measure of the mean distance between the borders of the segmented trabeculae).^{23,31,32} In line with the DEXA scan quantifications (Figure 2), the μ CT imaging of femurs from C- and V-treated mice revealed marked trabecular bone loss in young mice exposed to chemotherapy, consistent with decreased BV/TV (-82% , $P < .0001$), Tb.Th (-21% , $P < .05$), Tb.N (-80% , $P < .0001$), and Conn.Dn (-54% , $P < .01$), and with augmented Tb.Sp ($+61\%$, $P < .0001$) (Figure 4A). Representative 3D renderings also validated the outstanding loss of trabecular bone as measured by the μ CT analysis (Figure 4B).

Chemotherapy Induces Alterations in SMUP and MUNE

To validate prior findings that cachexia and chemotherapy can elicit impaired motor unit connectivity,³³⁻³⁵ we conducted

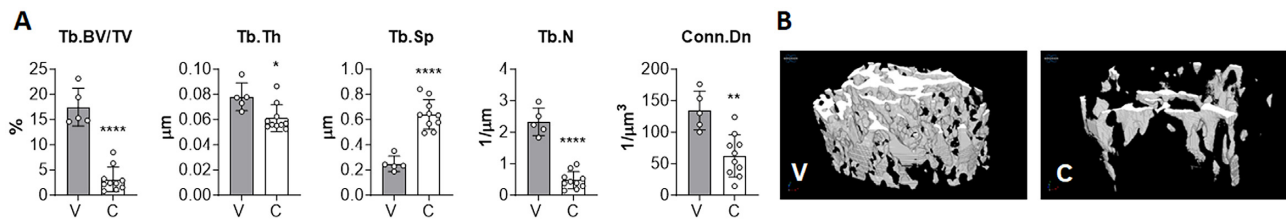


Figure 4. Chemotherapy profoundly affects trabecular bone. (A) Quantification of trabecular bone volume fraction (Tb.BV/TV; %), trabecular thickness (Tb.Th; μm), trabecular spacing (Tb.Sp; μm), trabecular number (Tb.N; $1/\mu\text{m}$), and connectivity density (Conn.Dn) in the femur of mice enrolled in experiment #1. Data reported as means \pm SD. Significant differences (* $P < .05$; ** $P < .01$; **** $P < .0001$) were determined by Student's *t*-test. (B) Representative μCT 3D image renders of femur sections in vehicle- and chemotherapy-treated mice.

electrophysiological assessments of 4-wk-old mice exposed to chemotherapy. In line with our previous findings¹⁵ baseline-to-peak CMAP assessment revealed no significant reductions between V and C groups (Figure 5A). Conversely, significant elevations in SMUP values were observed in the experimental group (+50%, $P < .0001$) compared to the controls (Figure 5B). In a similar manner, MUNE calculations revealed a decrease in motor unit number starting at week 2 and compounding through week 5 (W2: -40%, $P < .05$; W5: -54%, $P < .001$) (Figure 5C).

Folfiri Has a Profound Effect on Organ Weights

As shown previously by our lab, organs such as liver, spleen, gonadal fat, kidneys, and heart are perturbed by chemotherapy and cancer-induced cachexia.^{23,36} Mice that underwent chemotherapy had significantly smaller livers as compared to vehicle-treated mice (-15%, $P < .05$) (Figure S2A). Dissimilarly, spleen weights increased dramatically in the chemotherapy-treated group (+60%, $P < .05$) (Figure S2B). In agreement with our DXA scan values, the accumulation of gonadal fat in the young mice treated with Folfiri was significantly impaired compared to the control animals (-56%, $P < .001$) (Figure S2C). Kidneys also appeared smaller in weight due to chemotherapy (-27%, $P < .01$) (Figure S2D). Interestingly, chemotherapy seemed to have a minimal effect on heart size, similar to our initial observations in adult mice (Figure S2E).¹⁷

Body Growth Fails to Fully Recover After Cessation of Treatment

Given our observation that chemotherapy perturbs growth curve and body composition in young mice, we then investigated if the animals were able to recover after cessation of the treatment or whether chemotherapy-associated musculoskeletal abnormalities were persistent over time. Hence, in a second experimental cohort, 4-wk-old mice were administered Folfiri for 5 wk. After discontinuation of the treatment, the animals were monitored for changes in body composition and muscle function for up to 4 wk. Despite progressively attempting to gain back their body weight and close the initial gap with the V-treated animals (Figure 6A), at time of sacrifice (week 9), the mice exposed to Folfiri were still showing a significant body weight difference (-12%, $P < .0001$) (Figure 6B), which was reflected at level of carcass weight (-17%, $P < .0001$) (Figure 6C). Overall, when compared with the mice sacrificed at 5 wk, the recovered C-treated mice were only able to gain back ~3% of their weight compared to the respective controls (Table 1), and no significant differences were found in the average growth rates of V and C mice post cessation of treatment (V: 0.09 g/d; C: 0.13 g/d; data not shown). Interestingly, despite some acute

toxicity consequential to chemotherapy treatment, suggested by sudden drops in food intake (also in line with our previous observations),¹⁷ the cumulative food intake over the 9-wk experimental period was comparable between the V and C groups (205 g/mouse vs. 187 g/mouse, respectively; Figure S3). In particular, during the recovery phase, the food consumption for the C group fully rebounded, and both groups consumed roughly the same amount of food (Figure S3).

Abnormal Body Composition Persists Post-Cessation of Treatment

We then examined whether chemotherapy-induced changes in body composition (as shown in Figure 2) were corrected upon cessation of the treatment. BMD assessment displayed a lasting drop in the chemotherapy-treated group as compared to the controls at weeks 5 through week 9 (W5: -9%, $P < .0001$; W7: -8%, $P < .0001$; W9: -10%, $P < .0001$) (Figure 7A). Analogously, the BMC analysis showed persistently decreased values among groups, starting at week 5 (W5: -24%, $P < .0001$; W7: -17%, $P < .0001$; W9: -16%, $P < .0001$) (Figure 7A). The DEXA values for fat and lean mass quantification also continued to show persistent dysregulations, starting at 2 wk for fat (W2: -19%, $P < .001$; W5: -21%, $P < .0001$; W7: -14%, $P < .0001$; W9: -13%, $P < .0001$) and at 7 wk for lean mass (W7: -15%, $P < .05$; W9: -22%, $P < .0001$) (Figure 7B).

Skeletal Muscle Shows Partial Recovery Post Cessation of Folfiri

When compared to mice sacrificed at week 5 (Figure 3A), the recovered mice exhibited ~11% larger muscle mass on average across the 3 skeletal muscles collected (Table 1). However, the animals receiving Folfiri treatments exhibited persistently reduced gastrocnemius, quadriceps, and tibialis anterior muscle weights compared to the respective V-treated animals (-10%, $P < .001$; -14%, $P < .001$; -10%, $P < .001$, respectively) (Figure 8A). Further, in supplement of the sustained loss of skeletal muscle size, the C-treated mice also exhibited smaller myofiber CSA (-11%, $P < .05$ vs. V) (Figure S4). Plantarflexion torque assessments in the chemotherapy-administered mice revealed a sustained loss in muscle strength up to week 9 (W5: -19%, $P < .0001$; W7: -16%, $P < .001$; W9: -16%, $P < .0001$) (Figure 8B). Interestingly, when the *in vivo* muscle force assessment data were normalized to gastrocnemius weight at time of sacrifice, differences were lost between groups, thus showing that decreased muscle function is likely a result of smaller muscles (Figure S5). A main effect of treatment was seen in force production of the EDL muscle between the 2 groups ($P < .0001$), whereby the values of the C mice were consistently lower by an average of 13% vs. V

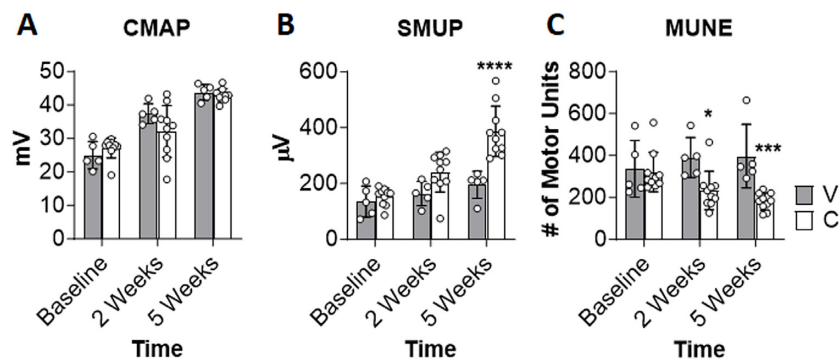


Figure 5. Chemotherapy induces alterations in single motor unit potential (SMUP) and motor unit number estimation (MUNE). (A) Compound muscle action potential (CMAP: millivolts (mV)), (B) SMUP (microvolts (μ V)), and (C) MUNE of the triceps surae muscles in 4-wk-old male mice treated with either vehicle or chemotherapy (experiment #1). Data reported as means \pm SD. Significant differences (* $P < .05$; *** $P < .001$; **** $P < .0001$) were determined using 2-way ANOVA.

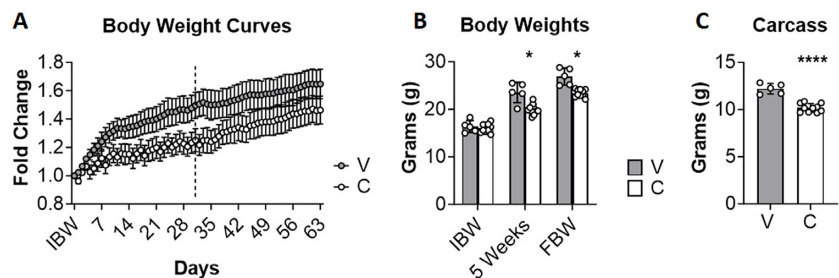


Figure 6. Body growth fails to fully recover after cessation of treatment. (A) Body weight change in mice enrolled in experiment #2, normalized to initial body weight (IBW). (B) Final body weights (FBW). (C) Carcass weights recorded after dissecting skeletal muscles and organs. Data reported as means \pm SD. Dashed line signifies the last treatment administered. Significant differences (**** $P < .0001$) were determined using Student's *t*-test and 2-way ANOVA.

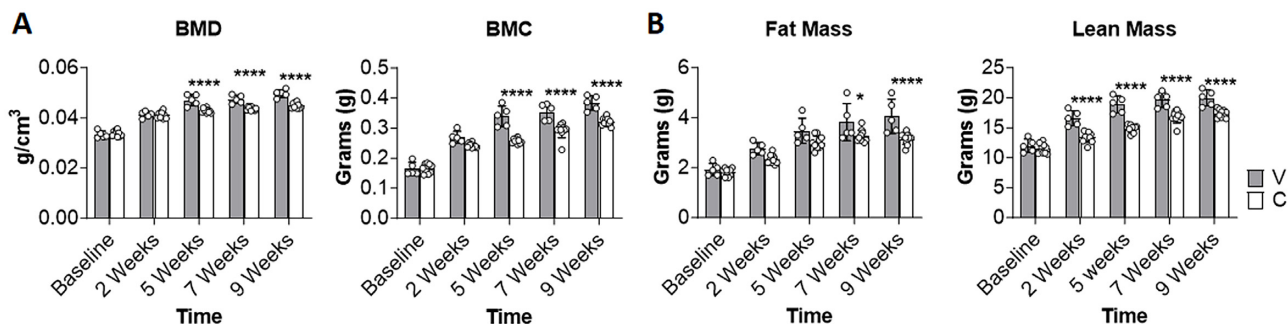


Figure 7. Abnormal body composition persists post-cessation of treatment. (A) Total bone mineral density (BMD), bone mineral content (BMC), (B) lean muscle mass, and fat mass assessed by dual-energy x-ray absorptiometry in mice from experiment #2. Data reported as means \pm SD. Significant differences (* $P < .05$; *** $P < .001$) were determined by using 2-way ANOVA.

(Figure 8C). Overall, when compared to the animals sacrificed at week 5 (Figure 3C), the recovered mice showed a \sim 7% increase in specific force of the EDL muscle (Table 1).

Trabecular Bone Shows Partial Recovery Post Cessation of Chemotherapy

Given our observations that chemotherapy acutely induces loss in trabecular bone in young animals, we sought to investigate the effects of Folfiri on bone mass after ceasing the treatment. Interestingly, trabecular bone was still significantly decreased in the C mice at time of sacrifice (week 9). Comparable to the mice sacrificed at 5 wk (Figure 4), decreases were observed in BV/TV (-49% , $P < .01$), Tb.N (-52% , $P < .001$), and Conn.Dn (-33% , $P < .01$) in the animals treated with chemotherapy and

allowed time to recover, whereas Tb.Sp was increased ($+57\%$, $P < .0001$) vs. the V-treated mice (Figure 9A). While the C-treated mice begin to recover trabecular bone by 4 wk post cessation of the treatment, exhibiting a 33% increase in total trabecular bone volume vs. the animals sacrificed at week 5, nonetheless it is also clear that trabecular deficits persist at week 9 (Table 1).

Levels of SMUP and MUNE Remain Altered Post Cessation of Chemotherapy

While it was previously shown that NMJs are altered due to chemotherapy, it remains unclear whether motor unit connectivity is rescued post cessation of treatment. Supporting our

Table 1. Percent difference between groups at 5 and 9 wk. Data reported as means \pm SD

	5 wk			9 wk		
	Vehicle raw values	Chemotherapy raw values	% difference	Vehicle raw values	Chemotherapy raw values	% difference
Body weights						
Final body weight	23.54 \pm 2.15	19.96 \pm 1.08	15%	26.90 \pm 1.78	23.43 \pm 0.79	12%
Carcass	10.16 \pm 1.12	8.60 \pm 0.34	15%	12.20 \pm 0.55	10.18 \pm 0.46	17%
Body composition						
BMD	0.05 \pm 0.002	0.04 \pm 0.002	5%	0.05 \pm 0.002	0.045 \pm 0.001	10%
BMC	0.32 \pm 0.04	0.29 \pm 0.02	11%	0.38 \pm 0.02	0.32 \pm 0.01	16%
Lean mass	17.94 \pm 0.82	15.32 \pm 0.15	15%	19.98 \pm 1.32	17.34 \pm 0.69	13%
Fat mass	2.58 \pm 0.76	2.25 \pm 0.44	18%	4.06 \pm 0.68	3.16 \pm 0.23	22%
Skeletal muscle mass						
Gastrocnemius	0.84 \pm 0.09	0.65 \pm 0.07	23%	0.90 \pm 0.08	0.81 \pm 0.07	10%
Quadriceps	0.997 \pm 0.14	0.77 \pm 0.07	23%	1.18 \pm 0.15	1.01 \pm 0.13	14%
Tibialis anterior	0.28 \pm 0.03	0.22 \pm 0.02	22%	0.31 \pm 0.03	0.28 \pm 0.02	10%
Muscle function						
Plantarflexion force	12.56 \pm 1.74	9.66 \pm .88	23%	14.22 \pm 1.73	11.89 \pm 1.19	16%
Specific force	339.30 \pm 96.01	269.20 \pm 75.94	21%	338.00 \pm 79.27	294.60 \pm 75.27	13%
Trabecular bone						
Tb.BV/TV	17.46 \pm 3.74	3.13 \pm 2.44	82%	13.42 \pm 4.40	6.856 \pm 2.97	49%
Tb.Th	0.08 \pm 0.01	0.06 \pm 0.01	21%	0.06 \pm 0.01	0.07 \pm 0.01	7%
Tb.Sp	0.25 \pm 0.06	0.64 \pm 0.12	61%	0.24 \pm 0.02	0.55 \pm 0.18	57%
Tb.N	2.33 \pm 0.43	0.48 \pm 0.27	80%	2.04 \pm 0.48	0.98 \pm 0.40	52%
Conn.D	134.40 \pm 30.75	62.43 \pm 33.50	54%	132.00 \pm 23.26	87.25 \pm 31.68	33%
Motor unit connectivity						
SMUP	194.72 \pm 29.45	386.45 \pm 118.20	50%	186.98 \pm 32.22	422.13 \pm 94.37	55%
MUNE	396.86 \pm 33.37	180.95 \pm 71.07	54%	341.67 \pm 59.76	152.87 \pm 38.00	55%
Organ weights						
Heart	0.84 \pm 0.16	0.71 \pm 0.12	15%	0.88 \pm 0.07	0.78 \pm 0.09	11%
Liver	7.10 \pm 0.57	6.03 \pm 0.77	15%	8.03 \pm 0.64	7.37 \pm 0.87	8%
Spleen	0.47 \pm 0.20	1.17 \pm 0.80	60%	0.41 \pm 0.01	0.47 \pm 0.09	13%
Fat	2.23 \pm 0.29	0.99 \pm 0.10	56%	2.45 \pm 0.48	1.88 \pm 0.14	23%
Kidney	1.04 \pm 0.20	0.76 \pm 0.80	27%	1.08 \pm 0.05	0.93 \pm 0.10	14%

Note: Percent differences were calculated between mean values for V- and C-treated groups at 5 and 9 wk.

earlier findings, baseline-to-peak levels of CMAP remained statistically unchanged across groups during and post treatment (Figure 10A). Interestingly, levels of SMUP seemed to remain elevated or even slightly increased in the chemotherapy group after cessation of the treatment (W2: +56%, $P < .01$; W5: +43%, $P < .01$; W7: +51%, $P < .001$; W9: +55%, $P < .0001$) (Figure 10B). Similarly, alterations of MUNE were slightly exacerbated after termination of chemotherapy administration, with significantly lowered levels observed starting at week 2 and persisting through week 9 (W2: -44%, $P < .0001$; W5: -38%, $P < .01$; W7: -48%, $P < .001$; W9: -55%, $P < .0001$) (Figure 10C). Notably, alterations in both SMUP and MUNE were more pronounced in mice sacrificed at week 9 than in those sacrificed at cessation of the 5-wk treatment (Table 1). To dive deeper into the molecular alterations associated with abnormal muscle innervation in the mice exposed to Folfiri, we assessed the expression of several NMJ components, in line with our previous studies.^{15,37} Significant reductions in protein levels were seen for MuSK (-34%, $P < .0001$), Rapsyn (-18%, $P < .05$), and Dok7 (-11%, $P < .05$) in the C-treated mice as compared to their respective controls (Figure 10D-G), thereby further supporting the idea that muscle innervation and motor unit connectivity remain altered post cessation of treatment.

Chemotherapy Perturbs Mitochondrial Homeostasis and Quality Control, while Stress-Related Response Proteins Remain Unchanged Post-Cessation of Treatment

We have previously shown that chemotherapy-induced muscle wasting drives upregulation of the ERK1/2 and p38 MAPK-dependent signaling.³⁸ Interestingly, in the present study, ERK1/2 remained unchanged (Figure 11A), while p38 was significantly down-regulated in the mice treated with chemotherapy (-34%, $P < .05$) (Figure 11B). We and others also showed that chemotherapy has profound effects on mitochondria, altogether leading to deficits in the overall energy metabolism.^{17,37} As we identified the effects of chemotherapy on muscle mass in young mice, we also examined the effects of chemotherapy on muscle mitochondrial homeostasis and quality control 4 wk post termination of treatment. Minimal alterations were seen in the expression of PGC-1 α (-10%, $P < .05$) when compared to the controls, whereas PGC-1 β remained substantially unchanged between groups (Figure 11C and D). Interestingly, we saw significant perturbations in VDAC expression in the chemotherapy group vs. the vehicle-treated mice (-28%, $P < .05$) (Figure 11E). Reductions in DRP-1 and OPA-1 levels, which we previously

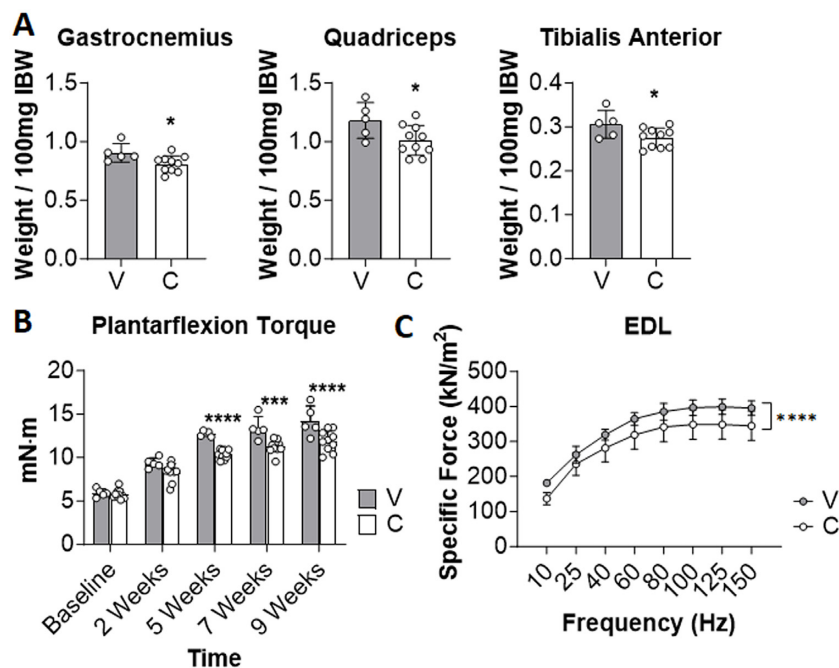


Figure 8. Skeletal muscle shows partial recovery post cessation of Folri. (A) Skeletal muscle weights from animals enrolled in experiment #2 were normalized to body weight at start of treatment (initial body weight—IBW). (B) In vivo plantarflexion torque assessment reported as absolute force (expressed as mN·m). (C) Ex vivo assessment reported as specific force (kN/m²). Data reported as means ± SD. Significant differences (**P* < .05; ****P* < .001; *****P* < .0001) were determined by Student's t-test and 2-way ANOVA.

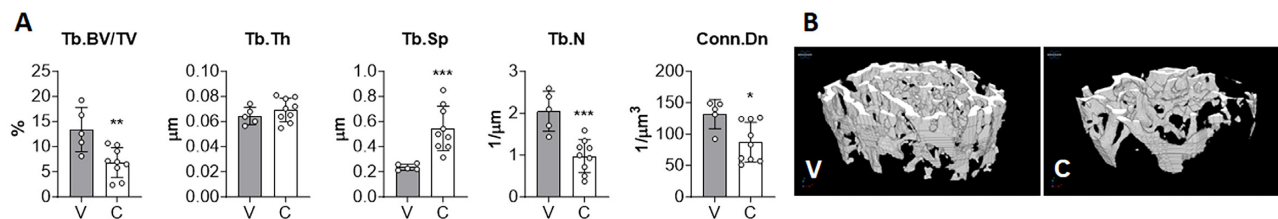


Figure 9. Trabecular bone shows partial recovery post-cessation of Folri. (A) Quantification of trabecular bone volume fraction (Tb.BV/TV; %), trabecular thickness (Tb.Th; μm), trabecular spacing (Tb.Sp; μm), trabecular number (Tb.N; 1/μm), and connectivity density (Conn.Dn) in the femur from mice enrolled in experiment #2. Data reported as means ± SD. Significant differences (**P* < .05; ***P* < .01; ****P* < .001) were determined Student's t-test. (B) Representative μCT 3D image renders of femur sections in vehicle and chemotherapy-treated mice.

reported following Folri treatment,⁸ were also found to persist following cessation of chemotherapy treatment (−18%, *P* < .01; 34%, *P* < .0001, respectively) (Figures 11F and G). No changes were seen between the groups for mitofusin-2 or cytochrome C (Figures 11H and I), whereas a decrease in COX IV was observed in the C-treated mice when compared to controls (−32%, *P* < .05) (Figure 11J). Moreover, consistent with the abnormal expression of proteins involved in the regulation of mitochondrial homeostasis, the SDH enzymatic activity was markedly reduced in the skeletal muscle from animals that underwent chemotherapeutic treatment (−60%, *P* < .0001) (Figure 11K).

Organs Show Potential for Partial Recovery Post Cessation of Treatment

Partial recovery was seen in organ weights post cessation of treatment. Mice that underwent chemotherapy maintained smaller livers post cessation of treatment (−8%, *P* < .05), with an increase in weight as compared to the first experiment, therefore showing potential for recovery (Figure S6A). Spleens in the chemotherapy-treated mice allowed time to recover followed

a similar, but less extreme increase (+13%, ns) (Figure S6B). The amount of gonadal fat in the mice treated with Folri and allowed to recover was still diminished, with a potential for partial recovery similar to previous DXA values (−23%, *P* < .01) (Figure S6C). Kidneys also saw a significant and persistent reduction in weight due to chemotherapy (−14%, *P* < .01) (Figure S6D). Administration of chemotherapy continued to promote minimal effect on cardiac muscles, with the comparable heart weights between the 2 experimental groups (−10%, ns) (Figure S6E).

Discussion

Studies from our group and others have shown that chemotherapy, when administered into adult rodents, induces skeletal muscle atrophy independent of cancer,¹⁵ whereas it contributes to exacerbating cachexia in the presence of a tumor, thus driving extensive metabolic complications and worsening skeletal muscle wasting and bone loss.^{39–41} Whether anticancer agents similarly impact muscle and bone in pediatric animals and whether these musculoskeletal complications persist even after discontinuation of the treatment remain to be elucidated. Analogously,

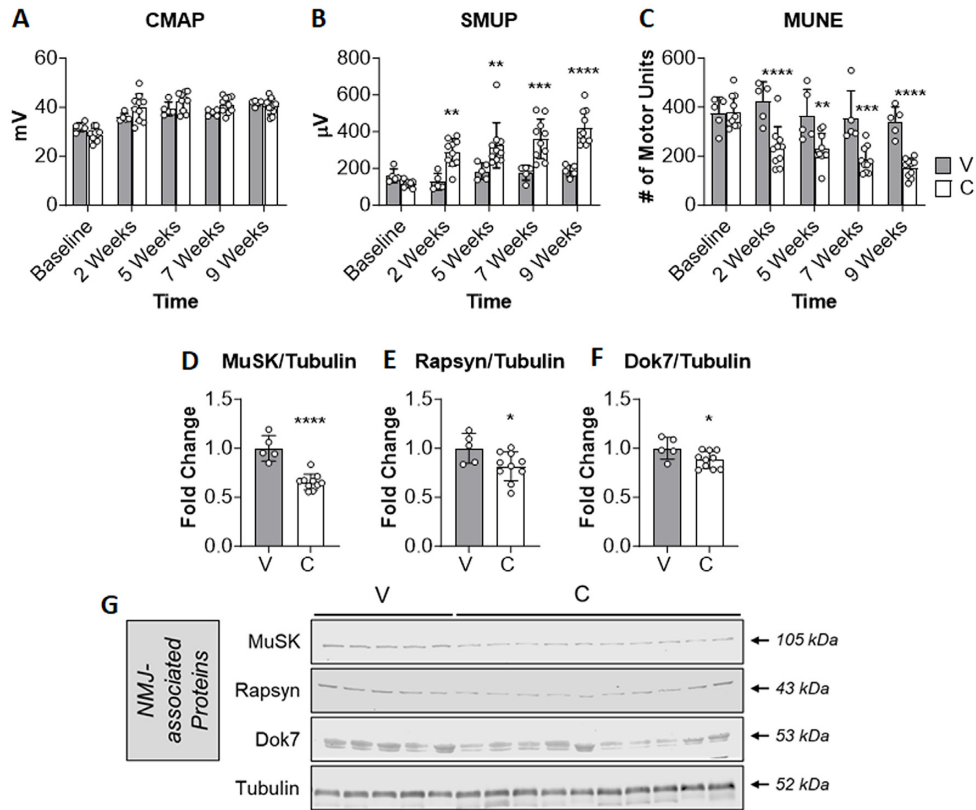


Figure 10. Muscle innervation remains altered post cessation of chemotherapy. (A) Compound muscle action potential (CMAP: millivolts (mV)), (B) single motor unit potential (SMUP: microvolts (μV)), and (C) motor unit number estimation (MUNE) of the *triceps surae* muscles in 4-wk-old male mice treated with either vehicle or chemotherapy (experiment #2). Quantification of protein expression (reported as fold change vs. Tubulin) for (D) MuSK, (E) Rapsyn, (F) Dok7, and (G) representative Western blotting images. Data reported as means ± SD. Significant differences (***P* < .01; ****P* < .001; *****P* < .0001) were determined using 2-way ANOVA.

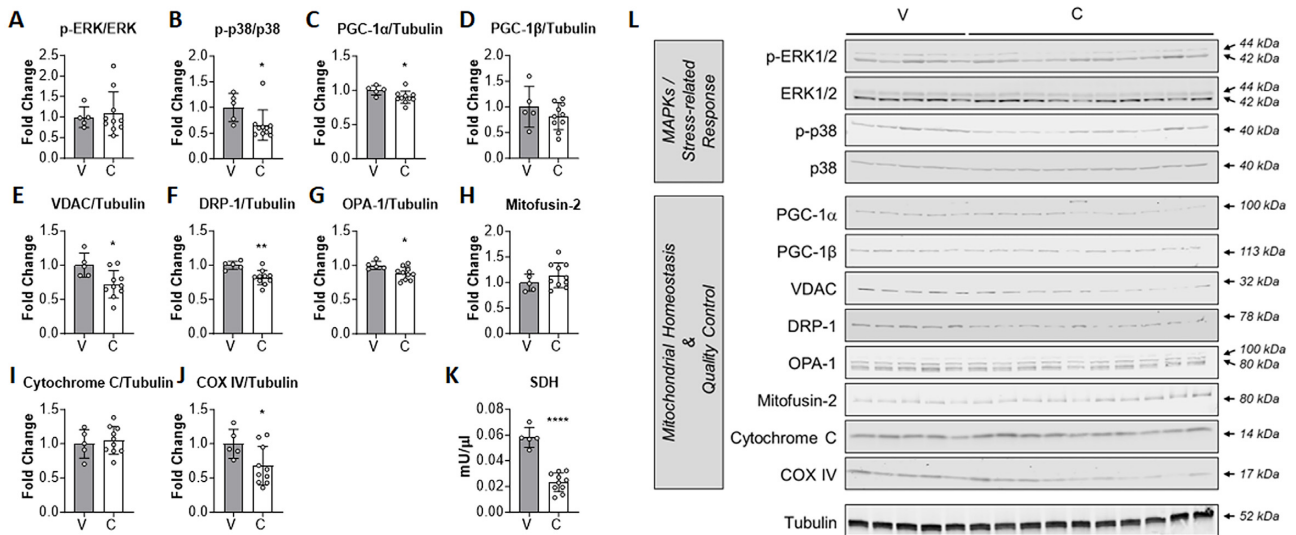


Figure 11. Chemotherapy perturbs mitochondrial homeostasis and quality control post-cessation of treatment. Quantification of protein expression (reported as a fold change vs. Tubulin) for (A) ERK1/2, (B) p38, (C) PGC-1α, (D) PGC-1β, (E) VDAC, (F) DRP-1, (G) OPA-1, (H) mitofusin-2, (I) cytochrome C, and (J) COX IV. (K) Muscle enzymatic activities of succinate dehydrogenase (SDH) in the soleus muscle, expressed in milliunits/μL (mU/μL). (L) Representative Western blotting images. Data reported as means ± SD. Significant differences (**P* < .05; ***P* < .01; *****P* < .0001) were determined by using Student's t-test.

the long-term musculoskeletal consequences of chemotherapy administration are poorly understood. Given that the average age of survival post diagnosis has been increasing in children with cancer due to new anti-cancer therapies and that these therapies are well known to induce cytotoxic responses in the host body, it has become increasingly important to understand the long-term effects of such treatments. Hence, the goal of our study was primarily to examine the late effects of chemotherapy when administered at a young age. Building upon our initial observations showing that the most debilitating side effects of chemotherapy in the host are skeletal muscle atrophy and weakness,^{8,9} our focus here was to look at critical body compositional elements such as bone, fat, lean mass, and muscle function in young animals administered anti-cancer agents.

Cancer-induced cachexia is a multi-organ wasting syndrome that is mainly characterized by loss of skeletal muscle mass, leading to muscle weakness and worsened survival in patients.^{3,10,11} Mechanisms that have been found to influence this multifactorial wasting syndrome include reduced anabolism, increased catabolism, abnormal muscle innervation, overproduction of reactive oxygen species (ROS), and decreased mitochondrial function, which altogether can lead to detrimental effects across many different tissues, organs, and cell types throughout the body.^{3,8,19} We and others highlighted similar mechanisms also in a setting of chemotherapy-induced cachexia, although protein hypercatabolism, generally accepted as a hallmark of cancer-induced muscle depletion, did not seem to play a major pathogenetic role.¹⁷ While our lab and others have shown that also chemotherapeutics directly promote skeletal muscle atrophy, weakness, weight loss, and other cachexia-like phenotypes, there is a general lack of data describing cachexia in the context of pediatric cancer, and the available animal models may not properly recapitulate the phenotype associated with the onset of acute cachexia in a child undergoing cancer treatment, nor its long-term musculoskeletal consequences. Hence, better and more representative animal models for the study of cachexia in pediatric age are desperately needed to further elucidate the mechanisms associated with the occurrence of musculoskeletal wasting in young mice.⁵

Our results indicate that Folfiri, a chemotherapy regimen widely utilized for the therapy of solid tumors,⁴² causes musculoskeletal defects in young mice that can persist for at least 4 wk after cessation of treatments. Here, we observed significant *in vivo* inhibition in muscle and bone growth up to 4 wk post cessation of a 5-wk chemotherapy treatment vs. the vehicle. Notably, comparing the animals from the second cohort with those sacrificed at cessation of treatment, an average 10% increase was seen in skeletal muscle weight, though the chemotherapy treated mice still displayed significantly smaller muscles than the controls at time of euthanasia. This data may seem to suggest that there is a potential for partial recovery in skeletal muscle mass post cessation of treatment. Interestingly, no recovery was seen in fat. These persistent adverse effects of chemotherapy are in line with findings on the late effects of radiotherapy, another widely utilized anti-cancer treatment, in adult survivors of pediatric cancer.⁴³ Indeed, in a clinical study performed examining children with various types of cancer and a median follow-up of 20 yr revealed that muscle atrophy was present in cancer survivors for up to 10 yr and fibrosis for up to 12 yr, whereas bone growth inhibition was visible for up to 15 yr post cessation of radiotherapy.⁴³ Analogously, studies in healthy mice treated with radiotherapy for rhabdomyosarcoma revealed a long-term decrease in myofiber size, myonuclear number, as well as a potential for lifelong fibrosis.^{44,45}

Here, we did not assess whether elevated fibrosis was evident in the skeletal muscle of rodents exposed to Folfiri, thus preventing us from generating conclusive observations in such regard. However, this data strongly suggests more detailed studies are needed to uncover long-lasting effects of anticancer therapies, especially since there is a lack of literature surrounding late effects of chemotherapy.

Survivors of pediatric cancer have been associated with increased risk of frailty, a condition marked by poor QoL, muscle weakness, low lean muscle mass, and low energy expenditure.^{43,46,47,48,49} As cachexia in adults is normally accompanied by muscle weakness concurrent to muscle depletion, we measured muscle function as an important means to test the strength of muscles in pediatric mice during and post cessation of treatment. Importantly, fatigue is one of the most frequently reported symptoms of childhood cancer survivors and can be indicative of decreased muscle function.^{49,50} Pediatric cancer patients also experience loss of motor function and reported physical limitations alongside neuromuscular deficits.⁵¹⁻⁵³ Our lab has previously reported that anti-cancer treatments such as cisplatin and Folfiri cause significant reductions in both absolute plantarflexion torque and specific force of EDL muscle.^{15,17,23} While our present study confirmed this loss in muscle function due to chemotherapy, it also showed that there is the potential to partially recover strength, as the *in vivo* data suggested that this recovery begins 2 wk after the cessation of treatment, with an average 3% increase in plantarflexion force. However, at time of sacrifice (week 9), the chemotherapy-treated animals still experienced significantly reduced muscle strength, suggesting a lasting effect on skeletal muscle function. Interestingly, Kallenbach et al. showed that radiotherapeutic treatment results in lifelong defects in myofiber size and myonuclear number.⁴⁴ Our study supports the idea that also chemotherapy is capable of eliciting long-term consequences to myofiber size, at least for 4 wk post cessation of therapy.

Our previous reports strengthened the idea that cachexia is a multifactorial and multiorgan syndrome impacting different organs and tissues. While ROS overproduction has been long known to contribute to the onset of cancer-induced cachexia, we have recently shown that elevated ROS levels also associate with muscle loss in rodents exposed to Folfiri.¹⁷ Interestingly, others have shown that excessive ROS production not only increases osteoclastogenesis, but also decreases osteoblastogenesis and osteoblastic activity, thus resulting in abnormal bone architecture and bone loss.⁵⁴ To attempt an explanation for the general stunted growth observed in our animals, despite negligible changes in food intake, we could also speculate that growth hormone deficiencies, as reported by Roman et al.⁵⁵ and by Haddy et al.⁵⁶ may take place following prolonged chemotherapy administration, thereby leading to a multiplicity of systemic effects. However, additional studies aimed at validating this hypothesis are needed.

Here, we showed that prolonged chemotherapy administration not only drives significant depletion of muscle and fat, but also bone. Bone loss, in particular, is an important clinical issue because of the drastically increased risk for fractures, as well as diminished QoL. We and others have shown that trabecular bone volume, number, and connectivity all are decrease consequential to chemotherapy treatments.³¹ Notably, the loss of BMD was also described in patients undergoing chemotherapy for various gynecologic cancer,^{57,58} whereas radiotherapy for abdominal tumors also triggered a substantial loss of BMD in patients with cancer.⁵⁹ In agreement with our previous studies performed in adult animals, in the current study, the

levels of BMC and BMD, as well as the trabecular bone mass, were found markedly decreased also in young mice following 5 wk of chemotherapy. Our data also highlighted the potential for partial recovery 4 wk after cessation of the treatment, although both BMC and BMD measurements, as well as the quantification of trabecular bone, were still exhibiting significant reductions compared to the vehicle-treated animals. Interestingly, Tb.Th a direct 3D measurement of average trabecular thickness within a selected volumetric area showed a complete recovery compared to the vehicle at the 4-wk timepoint after chemotherapy discontinuation, likely suggesting that thickness recovers as a protection against fracture before other trabecular measures.⁶⁰

Our group alongside others recently also reported that cancer and chemotherapy promote disruptions in NMJ homeostasis and protein levels, thereby leading to partial myofiber denervation, also suggestive of muscle atrophy.^{15,61} This dismantling of functionally connected motor units via cancer and chemotherapy can be seen through a decrease in the total MUNE and is capable of driving muscle weakness.^{15,33} The current study supports our previous findings that chemotherapy impairs motor unit connectivity, consistent with loss in MUNE, as well as with reduced MuSK, Rapsyn, and Dok-7 protein expression.^{15,37} Interestingly, this loss appears to be exacerbated in mice allowed time to recover from chemotherapeutic treatment by 17%, thus indicating that chemotherapy has a profound and long-lasting effect on the number of functionally connected motor units. While chemotherapy is well known to effectively promote reduced overall activity in mice, which in turn can lead to diminished muscle function as well as defective innervation,^{62,63} nonetheless, we did not assess the activity levels of mice before and after treatment, thereby preventing us from speculating on the effects of inactivity in the present experimental setting. The use of young, rapidly growing animals may have also contributed to increasing the discrepancies observed at the level of motor units among V- and C-treated mice, suggesting that denervation is likely an irreversible effect that can only be exacerbated as the individual grows. While this study did not specifically look at the molecular causes responsible for such stunning and persistent effects, especially on the motor units, we can speculate that the mitochondrial deficits may play a role. Indeed, our group has previously published that a generalized loss of mitochondria following cancer development or chemotherapy administration also associates with marked decreases in MUNE,^{15,37} whereas increasing mitochondrial biogenesis by boosting PGC-1 α levels in skeletal muscle was sufficient to preserve innervation and prevent NMJ defects. Interestingly, elevated ROS levels have also been reported in the muscle of mice treated with Folfiri.¹⁷ While ROS can be released as a consequence of mitochondrial dysfunctions, they have also been directly related to loss of both total motor units and muscle innervation.⁶⁴ Future studies will need to further elucidate the mechanistic relationship between mitochondria, ROS, and NMJs in order for targeted therapies to be developed.

While the musculoskeletal consequences of chemotherapy treatment resemble those of cancer, we showed that the molecular mechanisms responsible for the onset of skeletal muscle atrophy can be markedly different in adult animals exposed to Folfiri for up to 5 wk.^{3,8,15,17,24} Our group previously showed that an up-regulation in MAPK stress-related proteins such as ERK1/2 and p38 is associated with increased muscle wasting in mice exposed to chemotherapeutics.¹⁷ Interestingly, here the animals that were allowed time to recover from their treatment did not present with similar molecular alterations, likely due to the fact that, in the absence of chemotherapy, the muscles

were able to restore the normal levels of MAPK proteins. Of note, we reported that similar to cancer, chemotherapy drives dramatic mitochondrial alterations, likely contributing to muscle wasting and fatigue.^{3,9,17} Indeed, abnormal mitochondrial homeostasis and quality control have been directly related to the multifactorial nature of cachexia, and strategies aimed at preserving the muscle mitochondrial pool have been investigated as potential therapies against cancer- and chemotherapy-induced muscle wasting.^{3,38,65,66} As already mentioned above, these mitochondrial dysfunctions are known to drive skeletal muscle atrophy through oxidative and metabolic stress.^{3,21} Our observations here are consistent with our published work on mitochondrial stress induced by chemotherapy.¹⁷ Mitochondrial alterations corresponding with decreased expression of markers for mitochondrial fission and fusion were found in the chemotherapy treated group. In particular, decreases in markers such as PGC-1 α , DRP-1, OPA-1, COX IV, and VDAC, along with the abnormally reduced SDH activity, likely support the idea that mitochondrial quality control is disturbed by chemotherapeutics even after cessation of the treatment. Given that mitochondria are so closely tied to the onset of muscle wasting and weakness, therapies designed to foster mitochondrial recovery should be explored for survivors of childhood cancer.⁶⁵

Altogether, our data seems to suggest that musculoskeletal alterations persist post cessation of treatment, with at least a potential for partial recovery. While these observations are exciting per se, we must acknowledge a series of limitations of our study. First, our data shows that, unlike adult rodents, 4-wk-old mice exposed to chemotherapy do not present with actual loss of body and muscle mass, but rather exhibit stunted growth when compared to the respective vehicle-treated controls. While this is in line with clinical evidence highlighting growth hormone deficiency in childhood cancer survivors,⁶⁷ we cannot exclude that in this case the molecular mechanisms associated with appearance of muscle atrophy may differ from the canonical definition of cachexia. Furthermore, here we monitored mice for up to 4 wk post cessation of treatment. While this gave us a good indication of the persistent effects of chemotherapy on the musculoskeletal system, further studies will need to be performed including animals that are followed up for a longer period after treatment is concluded, at least up until when muscle and bone reach full maturation. The choice of chemotherapeutic to be tested may also represent a potential limitation of our study. Indeed, here we chose to use Folfiri because it is a commonly known chemotherapeutic agent that we have previously extensively characterized.^{3,8,15,17,23,24} Nonetheless, Folfiri is not commonly used to treat pediatric cancers, and therefore future studies will have to investigate the effects of more relevant chemotherapy drugs, alone or in combination with cancer. There were also slight differences in body composition between the first 5 wk of our 2 experiments. Indeed, while the first experiment saw a statistically significant change in the amount of gonadal fat compared to the V-treated mice beginning 2 wk after the start of the treatment, the second experiment did not exhibit fat loss until 2 wk post cessation of chemotherapy (week 7). While we cannot ignore these minimal differences, these can also be explained by natural variability when using experimental animals and overall, the trends in data remained unchanged. Lastly, in our study only male mice were investigated, primarily to maintain consistency with our previous studies characterizing the musculoskeletal defects following administration of chemotherapeutics.^{3,8,17} Given that on average, males 14-yr-old and younger statistically suffer from higher incidence rates of cancer,¹ prospective experiments will have to conclusively

determine whether young males and females respond differently to chemotherapy, in line with clinical observations generated in adults with cancer.^{68,69}

In conclusion, our study suggests that chemotherapeutic agents can induce musculoskeletal defects that are capable of persisting to later stages in life when administered in young, pediatric animals. We showed that Folfiri can elicit alterations in body weight, skeletal muscle, fat, and bone mass, along with muscle innervation deficits and abnormal mitochondrial homeostasis. Such effects persisted post cessation of treatment, although some potential for a partial recovery was observed. Interestingly, the effects related to muscle innervation seemed to worsen with time after discontinuation of the treatments, seemingly suggesting these are life-long, likely irreversible, defects. Future studies will have to further explore the molecular basis of these long-term side musculoskeletal complications so that new therapies to prevent or diminish chemotherapy related toxicities can be identified.

Acknowledgements

The #12G10 anti-Tubulin monoclonal antibody (developed by Frankel J and Nelsen EM at the University of Iowa) and the #MANDRA11 (8B11) anti-dystrophin monoclonal antibody (developed by Morris GE at the NE Wales Institute) were obtained from the Developmental Studies Hybridoma Bank, created by the NICHD of the NIH and maintained at the University of Iowa, Department of Biology, Iowa City, IA. The graphical abstract was created with BioRender.com.

Author Contributions

JRH and AB designed and supervised the study and interpreted the data. JRH, PDL, FP, CRT, CSC, NAJ, and AB acquired, analyzed, and interpreted the data. PDL drafted the manuscript. JRH, FP, CSC, NAJ, and AB edited and revised the manuscript. AB obtained the funding. All the authors approved the final edited version. The degree of contribution to the design, to performance of the experiments, and to manuscript writing were used to assign authorship order among co-first authors.

Supplementary Material

[Supplementary material](#) is available at the *APS Function* online.

Funding

This study was supported by the Department of Surgery and the Department of Otolaryngology—Head & Neck Surgery at Indiana University School of Medicine, the Department of Pathology and the Comprehensive Cancer Center at the University of Colorado Anschutz Medical Campus, and by grants from NIH/NIAMS (R01AR079379, R01AR080051) and ACS (132013-RSG-18-010-01-CCG) to AB. JRH, CSC, and NAJ were supported by T32 Institutional Training Grants from NIH/NIAMS and NIH/NCI (AR065971, AR080630, CA190216).

Conflict of Interest

None declared.

Data Availability

The data underlying this article will be shared on reasonable request to the corresponding author.

References

- 1 Ward E, DeSantis C, Robbins A, Kohler B, Jemal A. Childhood and adolescent cancer statistics, 2014. *CA Cancer J Clin*. 2014;**64**(2):83–103.
- 2 Siegel DA, Richardson LC, Henley SJ, et al. Pediatric cancer mortality and survival in the United States, 2001–2016. *Cancer*. 2020;**126**(19):4379–4389.
- 3 Pin F, Barreto R, Couch ME, Bonetto A, O’Connell TM. Cachexia induced by cancer and chemotherapy yield distinct perturbations to energy metabolism. *J Cachexia Sarcopenia Muscle*. 2019;**10**(1):140–154.
- 4 Damrauer JS, Stadler ME, Acharyya S, Baldwin AS, Couch ME, Guttridge DC. Chemotherapy-induced muscle wasting: association with NF- κ B and cancer cachexia. *Eur J Transl Myol*. 2018;**28**(2):7590.
- 5 Runco DV, Zimmers TA, Bonetto A. The urgent need to improve childhood cancer cachexia. *Trends Cancer*. 2022;**8**(12):976–979.
- 6 Pin F, Couch ME, Bonetto A. Preservation of muscle mass as a strategy to reduce the toxic effects of cancer chemotherapy on body composition. *Curr Opin Support Palliat Care*. 2018;**12**(4):420–426.
- 7 Dantzer R, Meagher MW, Cleeland CS. Translational approaches to treatment-induced symptoms in cancer patients. *Nat Rev Clin Oncol*. 2012;**9**(7):414–426.
- 8 Barreto R, Mandili G, Witzmann FA, Novelli F, Zimmers TA, Bonetto A. Cancer and chemotherapy contribute to muscle loss by activating common signaling pathways. *Front Physiol*. 2016;**7**:472.
- 9 Le Bricon T, Gugins S, Cynober L, Baracos V. Negative impact of cancer chemotherapy on protein metabolism in healthy and tumor-bearing rats. *Metabolism*. 1995;**44**(10):1340–1348.
- 10 Roeland EJ, Bohlke K, Baracos VE, et al. Management of cancer cachexia: ASCO guideline. *J Clin Oncol*. 2020;**38**(21):2438–2453.
- 11 Deans C, Wigmore SJ. Systemic inflammation, cachexia and prognosis in patients with cancer. *Curr Opin Clin Nutr Metab Care*. 2005;**8**(3):265–269.
- 12 Argilés JM, Busquets S, Stemmler B, López-Soriano FJ. Cancer cachexia: understanding the molecular basis. *Nat Rev Cancer*. 2014;**14**(11):754–762.
- 13 Fearon KC, Glass DJ, Guttridge DC. Cancer cachexia: mediators, signaling, and metabolic pathways. *Cell Metab*. 2012;**16**(2):153–166.
- 14 Melstrom L, Melstrom JK, Ding X, Adrian TE. Mechanisms of skeletal muscle degradation and its therapy in cancer cachexia. *Histol Histopathol*. 2007;**22**(7): 805–814.
- 15 Huot JR, Pin F, Bonetto A. Muscle weakness caused by cancer and chemotherapy is associated with loss of motor unit connectivity. *Am J Cancer Res*. 2021;**11**(6):2990–3001.
- 16 Bouma S. Diagnosing pediatric malnutrition: paradigm shifts of etiology-related definitions and appraisal of the indicators. *Nut in Clin Prac*. 2017;**32**(1):52–67.
- 17 Barreto R, Waning DL, Gao H, Liu Y, Zimmers TA, Bonetto A. Chemotherapy-related cachexia is associated with mito-

- chondrial depletion and the activation of ERK1/2 and p38 MAPKs. *Oncotarget*. 2016;7(28):43442–43460.
- 18 Pin F, Busquets S, Toledo M, et al. Combination of exercise training and erythropoietin prevents cancer-induced muscle alterations. *Oncotarget*. 2015;6(41):43202–43215.
 - 19 Argilés JM, López-Soriano FJ, Busquets S. Muscle wasting in cancer: the role of mitochondria. *Curr Opin Clin Nutr Metab Care*. 2015;18(3):221–225.
 - 20 de Vos-Geelen J, Fearon KC, Schols AM. The energy balance in cancer cachexia revisited. *Curr Opin Clin Nutr Metab Care*. 2014;17(6):509–514.
 - 21 Gilliam LA, St Clair DK. Chemotherapy-induced weakness and fatigue in skeletal muscle: the role of oxidative stress. *Antioxid Redox Signal*. 2011;15(9):2543–2563.
 - 22 Sultani M, Stringer AM, Bowen JM, Gibson RJ. Anti-inflammatory cytokines: important immunoregulatory factors contributing to chemotherapy-induced gastrointestinal mucositis. *Chemother Res Pract*. 2012;2012:490804.
 - 23 Barreto R, Kitase Y, Matsumoto T, et al. ACVR2B/Fc counteracts chemotherapy-induced loss of muscle and bone mass. *Sci Rep*. 2017;7(1):14470.
 - 24 O'Connell TM, Pin F, Couch ME, Bonetto A. Treatment with soluble activin receptor type IIB alters metabolic response in chemotherapy-induced cachexia. *Cancers*. 2019;11(9):222.
 - 25 Huot JR, Pin F, Narasimhan A, et al. ACVR2B antagonism as a countermeasure to multi-organ perturbations in metastatic colorectal cancer cachexia. *J Cachexia Sarcopenia Muscle*. 2020;11(6):1779–1798.
 - 26 Arnold WD, Sheth KA, Wier CG, Kissel JT, Burghes AH, Kolb SJ. Electrophysiological motor unit number estimation (MUNE) measuring compound muscle action potential (CMAP) in mouse hindlimb muscles. *JoVE (J Vis Exp)*. 2015;(103):e52899.
 - 27 Sheth KA, Iyer CC, Wier CG, et al. Muscle strength and size are associated with motor unit connectivity in aged mice. *Neurobiol Aging*. 2018;67:128–136.
 - 28 Schneider CA, Rasband WS, Eliceiri KW. NIH Image to ImageJ: 25 years of image analysis. *Nat Methods*. 2012;9(7):671–675.
 - 29 Bouxsein ML, Boyd SK, Christiansen BA, Guldberg RE, Jepsen KJ, Müller R. Guidelines for assessment of bone microstructure in rodents using micro-computed tomography. *J Bone Miner Res*. 2010;25(7):1468–1486.
 - 30 Niziolek PJ, Farmer TL, Cui Y, Turner CH, Warman ML, Robling AG. High-bone-mass-producing mutations in the Wnt signaling pathway result in distinct skeletal phenotypes. *Bone*. 2011;49(5):1010–1019.
 - 31 Essex AL, Pin F, Huot JR, Bonewald LF, Plotkin LI, Bonetto A. Bisphosphonate treatment ameliorates chemotherapy-induced bone and muscle abnormalities in Young Mice. *Front Endocrinol*. 2019;10:809.
 - 32 Hain BA, Xu H, Wilcox JR, Mutua D, Waning DL. Chemotherapy-induced loss of bone and muscle mass in a mouse model of breast cancer bone metastases and cachexia. *JCSM Rapid Commun*. 2019;2(1):1–12.
 - 33 Brown JL, Lawrence MM, Ahn B, et al. Cancer cachexia in a mouse model of oxidative stress. *J Cachexia Sarcopenia Muscle*. 2020;11(6):1688–1704.
 - 34 Daou N, Hassani M, Matos E, et al. Displaced myonuclei in cancer cachexia suggest altered innervation. *Int J Mol Sci*. 2020;21(3):1092.
 - 35 Huertas AM, Morton AB, Hinkey MJ, Ichinoseki-Sekine N, Smuder AJ. Modification of neuromuscular junction protein expression by exercise and doxorubicin. *Med Sci Sports Exerc*. 2020;52(7):1477.
 - 36 Huot JR, Pin F, Essex AL, Bonetto A. MC38 tumors induce musculoskeletal defects in colorectal cancer. *Int J Mol Sci*. 2021;22(3):486.
 - 37 Huot JR, Pin F, Chatterjee R, Bonetto A. PGC1 α overexpression preserves muscle mass and function in cisplatin-induced cachexia. *J Cachexia Sarcopenia Muscle*. 2022;13(5):2480–2491.
 - 38 Ballarò R, Lopalco P, Audrito V, et al. Targeting mitochondria by SS-31 ameliorates the whole body energy status in cancer- and chemotherapy-induced cachexia. *Cancers*. 2021;13(4):50.
 - 39 Daenen LG, Houthuijzen JM, Cirkel GA, Roodhart JM, Shaked Y, Voest EE. Treatment-induced host-mediated mechanisms reducing the efficacy of antitumor therapies. *Oncogene*. 2014;33(11):1341–1347.
 - 40 Middleton JD, Stover DG, Hai T. Chemotherapy-exacerbated breast cancer metastasis: a paradox explainable by dysregulated adaptive-response. *Int J Mol Sci*. 2018;19(11):333.
 - 41 Karagiannis GS, Condeelis JS, Oktay MH. Chemotherapy-induced metastasis: mechanisms and translational opportunities. *Clin Exp Metastasis*. 2018;35(4):269–284.
 - 42 Peeters M, Price TJ, Cervantes A, et al. Final results from a randomized phase 3 study of FOLFIRI \pm panitumumab for second-line treatment of metastatic colorectal cancer. *Ann Oncol*. 2014;25(1):107–116.
 - 43 Paulino AC. Late effects of radiotherapy for pediatric extremity sarcomas. *Int J Radiat Oncol Biol Phys*. 2004;60(1):265–274.
 - 44 Kallenbach JG, Bachman JF, Paris ND, et al. Muscle-specific functional deficits and lifelong fibrosis in response to paediatric radiotherapy and tumour elimination. *J Cachexia Sarcopenia Muscle*. 2022;13(1):296–310.
 - 45 Paris ND, Kallenbach JG, Bachman JF, et al. Chemoradiation impairs myofiber hypertrophic growth in a pediatric tumor model. *Sci Rep*. 2020;10(1):19501.
 - 46 Jóhannsdóttir IM, Hjermstad MJ, Moum T, et al. Increased prevalence of chronic fatigue among survivors of childhood cancers: a population-based study. *Pediatr Blood Cancer*. 2012;58(3):415–420.
 - 47 Ness KK, Howell CR, Bjornard KL. Frailty and quality of life in adult survivors of childhood cancer. *Expert Rev Qual Life Cancer Care*. 2017;2(2):79–85.
 - 48 Mulrooney DA, Ness KK, Neglia JP, et al. Fatigue and sleep disturbance in adult survivors of childhood cancer: a report from the childhood cancer survivor study (CCSS). *Sleep*. 2008;31(2):271–281.
 - 49 Ness KK, Leisenring WM, Huang S, et al. Predictors of inactive lifestyle among adult survivors of childhood cancer: a report from the Childhood Cancer Survivor Study. *Cancer*. 2009;115(9):1984–1994.
 - 50 Knobel H, Håvard Loge J, Lund MB, Forfang K, Nome O, Kaasa S. Late medical complications and fatigue in Hodgkin's disease survivors. *J Clin Oncol*. 2001;19(13):3226–3233.
 - 51 Söntgerath R, Eckert K. Impairments of lower extremity muscle strength and balance in childhood cancer patients and survivors: a systematic review. *Pediatr Hematol Oncol*. 2015;32(8):585–612.
 - 52 Beulertz J, Bloch W, Prokop A, Baumann FT. Specific deficit analyses in motor performance and quality of life of pediatric cancer patients—a cross-sectional pilot study. *Pediatr Hematol Oncol*. 2013;30(4):336–347.
 - 53 Hudson MM, Mertens AC, Yasui Y, et al. Health status of adult long-term survivors of childhood cancer: a report from the Childhood Cancer Survivor Study. *JAMA*. 2003;290(12):1583–1592.

- 54 Kimball JS, Johnson JP, Carlson DA. Oxidative stress and osteoporosis. *J Bone Joint Surg Am.* 2021;**103**(15):1451–1461.
- 55 Román J, Villaizán CJ, García-Foncillas J, Azcona C, Salvador J, Sierrasesúmaga L. Chemotherapy-induced growth hormone deficiency in children with cancer. *Med Pediatr Oncol.* 1995;**25**(2):90–95.
- 56 Haddy TB, Mosher RB, Nunez SB, Reaman GH. Growth hormone deficiency after chemotherapy for acute lymphoblastic leukemia in children who have not received cranial radiation. *Pediatr Blood Cancer.* 2006;**46**(2):258–261.
- 57 Christensen C, Cronin-Fenton D, Frøslev T, Hermann AP, Ewertz M. Change in bone mineral density during adjuvant chemotherapy for early-stage breast cancer. *Support Care Cancer.* 2016;**24**(10):4229–4236.
- 58 Lee SW, Yeo SG, Oh IH, Yeo JH, Park DC. Bone mineral density in women treated for various types of gynecological cancer. *Asia-Pac J Clin Oncol.* 2016;**12**(4):e398–e404.
- 59 Wei RL, Jung BC, Manzano W, et al. Bone mineral density loss in thoracic and lumbar vertebrae following radiation for abdominal cancers. *Radiother Oncol.* 2016;**118**(3):430–436.
- 60 Parfitt AM. Trabecular bone architecture in the pathogenesis and prevention of fracture. *Am J Med.* 1987;**82**(1):68–72.
- 61 Sartori R, Hagg A, Zampieri S, et al. Perturbed BMP signaling and denervation promote muscle wasting in cancer cachexia. *Sci Transl Med.* 2021;**13**(605):eaay9592.
- 62 Misiąg W, Piszczyk A, Szymańska-Chabowska A, Chabowski M. Physical activity and cancer care—a review. *Cancers.* 2022;**14**(17):154.
- 63 Bodine SC. Disuse-induced muscle wasting. *Int J Biochem Cell Biol.* 2013;**45**(10):2200–2208.
- 64 Vasilaki A, Richardson A, Van Remmen H, et al. Role of nerve-muscle interactions and reactive oxygen species in regulation of muscle proteostasis with ageing. *J Physiol.* 2017;**595**(20):6409–6415.
- 65 Pin F, Huot JR, Bonetto A. The mitochondria-targeting agent MitoQ improves muscle atrophy, weakness and oxidative metabolism in C26 tumor-bearing mice. *Front Cell Dev Biol.* 2022;**10**:861622.
- 66 Huot JR, Baumfalk D, Resendiz A, Bonetto A, Smuder AJ, Penna F. Targeting mitochondria and oxidative stress in cancer- and chemotherapy-induced muscle wasting. *Antioxid Redox Signal.* 2023;**38**(4-6):352–370.
- 67 Pollock NI, Cohen LE. Growth hormone deficiency and treatment in childhood cancer survivors. *Front Endocrinol.* 2021;**12**:745932.
- 68 Wagner AD. Sex differences in cancer chemotherapy effects, and why we need to reconsider BSA-based dosing of chemotherapy. *ESMO Open.* 2020;**5**(5):e000770.
- 69 Rose TL, Deal AM, Nielsen ME, Smith AB, Milowsky MI. Sex disparities in use of chemotherapy and survival in patients with advanced bladder cancer. *Cancer* 2016;**122**(13):2012–2020.